Atlas of Clinical Cases on Brain Tumor Imaging

Yelda Özsunar
Utku Şenol
Editors

Springer

Atlas of Clinical Cases on Brain Tumor Imaging

Yelda Özsunar • Utku Şenol
Editors

Atlas of Clinical Cases on Brain Tumor Imaging

Springer

Editors
Yelda Özsunar
Radiology Department
Adnan Menderes University
Aydın
Turkey

Utku Şenol
School of Medicine
Akdeniz University
Antalya
Turkey

ISBN 978-3-030-23272-6 ISBN 978-3-030-23273-3 (eBook)
https://doi.org/10.1007/978-3-030-23273-3

This Springer imprint is published by the registered company Springer Nature Switzerland AG
The registered company address is: Gewerbestrasse 11, 6330 Cham, Switzerland

Preface

With our well-known and accomplished authors who are competent in their fields, we believe that we have prepared a book which will be found interesting and beneficial about brain tumors.

Brain tumors are one of the most challenging diseases of neuroradiology not only in terms of diagnosis but also in management aspect. For example, glioblastomas (GBM), which encounter about half of the glial tumors, are still one of the most deadly tumors, despite the significant development of molecular and imaging technologies and advanced therapy methods.

In the last three decades, survival rates for GBM have shown no notable improvement. Therefore, we believe that the integration of most recent developments, such as genomic knowledge with clinical and imaging experience, might potentially improve the management of this devastating disease. In most cases, decision-making in diagnosis and therapy is complex and needs close interdiciplinary teamwork. Therefore, we tried to accomplish a multidiciplinary approach for preparing this book. We presented our book in two parts: The first part is the general, multidiciplinary explanation of most recent developments and basic knowledge about the brain tumors. The second part represents several imaging samples of brain tumors with brief but important explanations.

Translation of pathological and clinical findings to a simple and illustrative teaching tool is very important. Most radiologists and clinicians prefer not too complex and straightforward information with many cases presented with images. Simple pathological findings, such as increased neovascularity, should be easily translated into the dictionary of radiologist as increased perfusion and should be presented with numerous illustrations to enhance experience and knowledge of the interpreter. Therefore, this book will be a very useful and quick reference for primarily radiologists, neuroradiologists,

oncologists, radiation oncologists, neurosurgeons, and pathologists. The book also includes the most recent development of the imaging technology, management strategies, and pathological classifications.

In short, as editors and authors, we expected to present this book as a quick reference with brief and important illustrative explanations of brain tumors. The most recent multidiciplinary technical, clinical, molecular, and genetic developments have been also explained with simple explanations and images. We hope that this book will serve as a pleasant, informative, quick, and useful book in clinics of different disciplines which study brain tumors.

Aydın, Turkey — Yelda Özsunar
Antalya, Turkey — Utku Şenol

Contents

Part I

General Considerations in Brain Tumors

1 Pathology, Epidemiology, and WHO Classification of Brain Tumors

Özlem Yapıcıer

1.1 Epidemiology and Pathology of the Central Nervous System Tumors

The incidence of all brain tumors is reported to be ranged from 4.3 to 18.6 per 100,000 person-years [1]. Primary brain tumors constitute 50–75% of all central nervous system (CNS) tumors whereas secondary brain tumors, majority of which are carcinoma metastases, occur in the remaining 25–50%.

Although relatively rare in adults, primary CNS tumors are the most common type of solid tumors in infants and children. Pediatric CNS tumors differ from their adult counterpart with regard to the histological type and site of occurrence. For instance, the majority of the tumors occur in the supratentorial compartment in adults, whereas the infratentorial compartment is the most common site in the pediatric population. Regarding the tumor histology, the most common type encountered in adults is meningioma, followed by glioma, half of which being glioblastoma, and pituitary adenoma. On the other hand, the most common type seen in the pediatric population is glioma, majority of which is pilocytic astrocytoma, and embryonal tumors among which medulloblastoma is the leading type.

Ö. Yapıcıer (✉)
Department of Pathology, School of Medicine, Bahcesehir University, Istanbul, Turkey
e-mail: ozlem.yapicier@med.bau.edu.tr

Primary spinal cord tumors constitute 5–12% of all primary CNS tumors. Of these, 85% are extramedullary, with schwannoma and meningioma being the most common types. Intramedullary tumors, majority of which are ependymomas and astrocytomas, are much rarer. Regarding the metastatic spinal tumors, the most common primary malignancy in adults is lung cancer (adenocarcinoma in particular), followed by breast cancer, melanoma, renal cell carcinoma, and colorectal cancer. In the pediatric population, leukemia and lymphoma are the most common types of the metastatic tumors, followed by germ cell tumors, osteosarcoma, neuroblastoma, Ewing sarcoma, and rhabdomyosarcoma. Metastasis to the spinal cord, which constitutes 8–9% of spinal metastases, arises from the vertebral body or via direct infiltration from the paravertebral tissues. The most common culprit for intramedullary metastasis is small cell lung cancer, whereas for the spinal epidural disease, it is the prostate, breast, and lung.

CNS tumors arise from a number of different tissues that consist of various cell types, such as the brain parenchyma, the ventricles, pineal and sellar region, cranial and spinal nerves, and meninges. This is why CNS tumors are a very large and heterogenous group of tumors. A number of potential risk factors have been investigated in epidemiological studies with regard to the development of CNS tumors. Among these, ionizing radiation and genetic tendency have been shown to have a stronger correlation.

Y. Özsunar, U. Şenol (eds.), *Atlas of Clinical Cases on Brain Tumor Imaging*,
https://doi.org/10.1007/978-3-030-23273-3_1

However, although some brain tumor types occur in people with familial tumor syndromes such as neurofibromatosis or Li-Fraumeni syndrome, it is known that 95% of brain tumors are sporadic. Likewise, brain tumors may occur in individuals exposed to ionizing radiation; however, the majority of brain tumor patients have no history of prior ionizing radiation. Large epidemiological studies based on clinicopathological research are likely to shed more light on the immunological, genetic, and other potential risk factors that are likely to play a role on the development of CNS tumors.

1.2 An Overview of the WHO Classifications of Tumors of the Central Nervous System

The first edition of the "World Health Organization (WHO) Classification of Tumors of the Central Nervous System" published in 1979 was based mainly on the histogenesis of the tumors depending on their light microscopic features in routine hematoxylin and eosin-stained sections [2]. Since then, four classification updates have been published in 1993, 2000, 2007, and 2016, the last being the revised version of the 2007 edition (4th edition) rather than a new formal edition [3–6].

In the 1993 classification, immunohistochemical expressions of relevant proteins were added to the diagnostic algorithm in addition to histopathologic features. Although subsequent classifications of 2000 and 2007 put an emphasis on genetic factors in tumorigenesis as a result of greatly increased knowledge of the genetic basis of brain tumors, these not fully understood genetic changes fell short in specifying the tumors in the mentioned classifications. Through new genetic discoveries, the recent 2016 classification has been structured with a better understanding of the role of these genetic alterations play in prognosis and treatment response. In this context, the most important development in the field since the previous edition of the WHO classification 2007 has been the discovery of somatic mutations in the gene encoding isocitrate dehydrogenase (IDH) in adult diffuse gliomas. Sanson et al. [7] showed that diffuse gliomas in adults which do not contain IDH mutation show a more aggressive clinical behavior independent of the WHO grade. In 2014, the International Society of Neuropathology formulated guidelines [8] on how to incorporate molecular findings into CNS tumor classification. The proposed integrated diagnosis scheme was composed of four layers; Layer 2 containing the histological classification, Layer 3 tumor grade, and Layer 4 molecular information, while Layer 1 generating the integrated diagnosis by combining all the data from the other three layers. This "integrated" approach provided the fundamentals for the current classification. As such, the 2016 classification has emerged as one that builds biologically more homogeneous diagnostic categories by integrating well-established genotypic parameters along with phenotypic features.

1.3 Major Differences of WHO 2016 Classification

- The most significant changes took place in the category of glial neoplasms (Table 1.1) when compared to WHO 2007 classification [5]. All diffusely infiltrating gliomas whether astrocytic or oligodendroglial were grouped together based on their shared IDH gene mutation status along with the shared growth pattern and behaviors. Astrocytomas that lack IDH gene family mutations but with frequent BRAF alterations or tuberous sclerosis complex (TSC1/TSC2) mutations and circumscribed growth pattern were grouped separately from diffuse gliomas as "other astrocytic tumors." Molecular assay findings were incorporated into the diagnosis of diffuse gliomas as an extension of histopathological diagnosis (e.g., diffuse astrocytoma, IDH mutant)
- Medulloblastomas were reclassified as mutually complementary two broad groups containing genetically and histopathologically

Table 1.1 The comparison of 2007 and 2016 WHO CNS tumor classifications for glial neoplasms

2007—Glial neoplasms			2016—Glial neoplasms		
Astrocytomas	Oligodendrogliomas and oligoastrocytic tumors	Ependymomas	Diffuse astrocytic and oligodendroglial tumors	Other astrocytic tumors	Ependymal tumors
Diffuse astrocytomas Fibrillary[a] Gemistocytic Protoplasmic[a]	Oligodendroglioma	Subependymoma	Diffuse astrocytoma, ***IDH-mutant*** Gemistocytic astrocytoma, ***IDH-mutant*** ***Diffuse astrocytoma, IDH-wild type*** Diffuse astrocytoma, ***NOS***	Pilocytic astrocytoma Pilomyxoid astrocytoma	Subependymoma
Anaplastic astrocytoma	Anaplastic oligodendroglioma	Myxopapillary ependymoma	Anaplastic astrocytoma, ***IDH-mutant*** ***Anaplastic astrocytoma, IDH-wild type*** Anaplastic astrocytoma, ***NOS***	SEGA	Myxopapillary ependymoma
Glioblastoma Giant cell Gliosarcoma	Oligoastrocytoma	Ependymoma Cellular ependymoma[a] Papillary ependymoma Clear cell ependymoma Tanycytic ependymoma	Glioblastoma, ***IDH-wild type*** Giant cell glioblastoma Gliosarcoma ***Epithelioid glioblastoma*** Glioblastoma, ***IDH-mutant*** Glioblastoma, ***NOS***	PXA	Ependymoma Papillary ependymoma Clear cell ependymoma Tanycytic ependymoma
Gliomatosis cerebri[a]	Anaplastic oligoastrocytoma	Anaplastic ependymoma	***Diffuse midline glioma, H3 K27M mutant***	***Anaplastic PXA***	***Ependymoma, RELA fusion-positive***
Pilocytic astrocytoma Pilomyxoid astrocytoma			Oligodendroglioma, ***IDH-mutant/1p19q codeleted*** Oligodendroglioma, ***NOS***		Anaplastic ependymoma
SEGA			Anaplastic oligodendroglioma, ***IDH-mutant and 1p19q codeleted*** Anaplastic oligodendroglioma, ***NOS***		
PXA			Oligoastrocytoma, ***NOS*** Anaplastic oligoastrocytoma, ***NOS***		

IDH isocitrate dehydrogenase, *NOS* not otherwise specified, *SEGA* subependymal giant cell astrocytoma, *PXA* pleomorphic xanthoastrocytoma
Italicized terms: New designations
[a]Not included into the new (2016) classification

Table 1.2 2016 WHO classification of medulloblastomas

Medulloblastomas, histologically defined
Medulloblastoma, classic
Desmoplastic/nodular medulloblastoma
Medulloblastoma with extensive nodularity
Large cell/anaplastic medulloblastoma
Medulloblastomas, genetically defined
Medulloblastoma, WNT-activated
Medulloblastoma, SHH-activated and TP53-mutant
Medulloblastoma, SHH-activated and TP53-wild type
Medulloblastoma, non-WNT/non-SHH
Medulloblastoma, group 3
Medulloblastoma, group 4

Table 1.3 New entities, variants and patterns included in the 2016 WHO classification

Entities
Genetically defined diffuse gliomas
Glioblastoma, IDH-wild type, and IDH-mutant
Diffuse midline glioma, H3 K27M-mutant
Ependymoma, *RELA* fusion-positive
Genetically defined medulloblastomas
Embryonal tumor with multilayered rosettes (ETMR), C19MC-altered
Anaplastic pleomorphic xanthoastrocytoma
Diffuse leptomeningeal glioneuronal tumor
Variants
Epithelioid glioblastoma
Patterns
Glioblastoma with primitive neuronal component
Multinodular and vacuolating neuronal tumor of the cerebrum

defined tumors (Table 1.2). Anaplastic and large cell variants of medulloblastoma were combined as a single entity with two different morphological features of the same spectrum in the 2016 WHO classification

- The group of embryonal tumors of the CNS was reconstructed with the incorporation of genetically defined entities. Medulloepithelioma, CNS neuroblastoma, CNS ganglioneuroblastoma, and CNS embryonal tumor, NOS were grouped together as "other CNS embryonal tumors" since no specific genetic alteration has been shown pertaining to them yet. Ependymoblastoma, a separate entity under the embryonal tumors group in the 2007 classification, was regarded as one of the three histological patterns of embryonal tumor with multilayered rosettes (ETMRs), C19MC-altered in the current classification, on the basis of their molecular commonality. The primitive neuroectodermal tumor was removed from the classification
- Newly recognized entities, variants, and patterns were included in the current classification (Table 1.3)
- Some entities and variants were excluded from the classification. Fibrillary astrocytoma, protoplasmic astrocytoma, gliomatosis cerebri, cellular ependymoma, and primitive neuroectodermal tumor are no longer present in 2016 WHO classification. Gliomatosis cerebri, on the other hand, was considered merely as a growth pattern rather than being a distinct entity. Although this extensive involvement pattern of the neuroaxis can be seen in all subtypes of diffuse glioma, it is most commonly seen in anaplastic astrocytoma
- Chordoid glioma of the third ventricle, angiocentric glioma, and astroblastoma were grouped under "other gliomas" in 2016, not under the heading of "other neuroepithelial tumors" as in 2007 WHO classification
- Brain invasion was included as a criterion for the diagnosis of atypical meningioma
- Solitary fibrous tumor and hemangiopericytoma (SFT/HPC) were reconstituted as one entity and a new grading system as Grade I–II–III has been adapted for this entity
- The group of nerve sheath tumors was expanded by the addition of atypical neurofibroma, hybrid nerve sheath tumors, and malignant peripheral nerve sheath tumor with perineurial differentiation. Melanotic schwannoma was separated from other schwannomas
- The group of hematopoietic/lymphoid tumors was expanded in accordance with the changes in the classification of systemic lymphomas and histiocytic neoplasms over the past decade
- Pediatric diffuse gliomas showing similar histopathological features with their adult counterparts are addressed as separate entities due to a number of important differences

  - *Pediatric diffuse astrocytic tumors*: These tumors were shown to possess different clinicopathological (incidence, site, anaplastic progression) and genetic features as compared to the adult type. These include MYB and BRAF alterations, whereas the adult types harbor IDH1, IDH2, TP53, and ATRX mutations
  - *Pediatric high-grade diffuse astrocytic tumors*: Pediatric anaplastic astrocytoma (WHO Grade III) and glioblastoma (WHO Grade IV) were combined as a single category owing to the therapeutic implications. Like the low-grade counterparts, these tumors also show clinicopathological and genetic differences as compared to the adult types. One entity, which shows only H3F3A or K27M mutation on HIST1H3B/C and is mainly seen in the pediatric population and at sites like the spinal cord and midline structures such as the thalamus and the brainstem is included in the classification as a separate entity named "Diffuse midline glioma, H3 K27M-mutant"
  - *Pediatric-type oligodendroglioma* (oligodendroglioma lacking IDH mutation and 1p19q codeletion): These tumors were shown to constitute the majority of oligodendrogliomas in children and adolescents. It is emphasized that with the aid of molecular studies, these tumors could be distinguished from histopathologically similar tumors which show round cell morphology, such as the dysembryoplastic neuroepithelial tumor, angiocentric glioma, pilocytic astrocytoma, and extraventricular neurocytoma
- The term "oligoastrocytoma" is discouraged in the current classification since the use of both genotypical and phenotypical studies in these tumors results in more homogeneously defined categories as either astrocytoma or oligodendroglioma. With a simplified genotypic approach, IDH-mutant, *ATRX*-mutant, and 1p/19q-intact tumors are distinctively astrocytic while IDH-mutant, *ATRX*-wild-type, and 1p/19q-codeleted tumors are oligodendroglial
- No direct relevance between grade and biological behavior has been established in ependymomas to date [9, 10]. Consequently, the issue of the subjective nature of the histopathological criteria used in the classification of classical ependymoma (WHO Grade II) and anaplastic ependymoma (WHO Grade III) still remained in the most recent classification. A recent study by Pajtler et al. [11] suggests that ependymomas occurring in three principal anatomical locations have different genetic alterations and prognoses and utilizing transcriptome and methylome profiling might serve as the basis of molecular classification for ependymomas. However, for the time being, the only genetically defined subtype is *RELA* fusion-positive ependymoma constituting the majority of supratentorial tumors of childhood
- *Grade*:
  - Three grades were defined for the solitary fibrous tumor/hemangiopericytoma. The idea of a single entity encompassing different grades is not new for the tumors outside of the central nervous system. However, this is the first time this notion is introduced for central nervous system tumors
  - The majority of the diffuse leptomeningeal glioneural tumors, which has been recently included in the classification, are low-grade lesions. However, as a result of limited patient size and insufficient clinical follow-up, a grading has not been proposed for these tumors yet
  - Pilomyxoid astrocytomas show a wide spectrum of biological behavior. However, they do have a higher tendency for recurrence or cerebrospinal dissemination as compared to pilocytic astrocytomas. Since it is still not clear whether this aggressive behavior is a result of some inherent biological features or simply the unfavorable hypothalamic/chiasmatic location, a grading has not been applied to them
- *"NOS"* (not otherwise specified) designation is added to the diagnostic categories as an extension of the histopathological diagnosis when genetic testing is not done or done but is inconclusive

1.4 Diagnostic Algorithm Based on the 2016 CNS Tumor Classification

In this recent classification, some tumor groups are diagnosed by the combination of histomorphological and molecular/genetic features while many tumor groups are still diagnosed mainly by microscopic morphologic features. The former is predominantly used in diffuse astrocytic/oligodendroglial tumors and medulloblastoma categories.

1.4.1 Diffuse Astrocytic and Oligodendroglial Tumors

Although it is not necessary to follow a certain sequence, the first step recommended in the diagnosis algorithm of this tumor group in adults is to define the histomorphological subtype of diffuse glioma, followed by genetic testing for IDH status and 1p19q codeletion as depicted below and in Table 1.4.

1. Histomorphology: Astrocytoma, oligodendroglioma, oligoastrocytoma, or glioblastoma
2. IDH status: IDH mutant or IDH wild type
3. 1p19q codeletion: Presence or absence of 1p19q codeletion

Presence of 1p19q codeletion is essential in IDH mutated diffuse gliomas for the diagnosis of oligodendroglioma. Other genetic parameters including *ATRX* loss and TP53 mutation are characteristic but not required for the diagnosis of diffuse astrocytomas. Lack of nuclear ATRX immunoexpression is characteristic for astrocytomas while oligodendrogliomas have nuclear ATRX immunoexpression (Figs. 1.1 and 1.2).

However, if genetic tests are readily accessible, molecular/genetic data may precede histomorphological assessment throughout the course of integrated diagnosis.

IDH: Since the isocitrate dehydrogenase mutation has become a definitive marker for the adult diffuse glial tumors in the recent classification, it constitutes an important part of the diagnostic algorithm. Only IDH1 and IDH2 mutations, which are two of the three isoforms of IDH, have been detected in human gliomas. Mutations in the IDH1 isoform are much more common than those in the IDH2 isoform. IDH1 mutations are the earliest detectable genetic alteration in low-grade diffuse astrocytomas and in all oligodendrogliomas and also seen in secondary glioblastomas, which progress from a precursor diffuse astrocytoma or anaplastic astrocytoma [12]. The most frequent IDH1 mutation found in almost 90% of astrocytic and oligoden-

Table 1.4 Diagnostic algorithm for adult diffuse astrocytic and oligodendroglial tumors

Histomorphology	IDH status	1p19q codeletion	Diagnosis
Astrocytoma	Mutant	Absent	Diffuse astrocytoma, IDH mutant
	Wild type	Absent	Diffuse astrocytoma, IDH wild type
	Not done/ inconclusive	Absent	Diffuse astrocytoma, NOS
Oligodendroglioma	Mutant	Present	Oligodendroglioma, IDH mutant, 1p19q codeleted
	Wild type	No need to apply	Oligodendroglioma, NOS (after exclusion of histological mimics[a])
	Not done/ inconclusive	Not done/ inconclusive	Oligodendroglioma, NOS
Oligoastrocytoma	Very rare. Restricted to mixed gliomas with dual-genotype		
Glioblastoma	Mutant	No need to apply	Glioblastoma, IDH mutant (secondary glioblastoma)
	Wild type	No need to apply	Glioblastoma, IDH wild type (primary glioblastoma)
	Not done/ inconclusive	No need to apply	Glioblastoma, NOS

[a]Neurocytoma, dysembryoplastic neuroepithelial tumor, clear cell ependymoma, pilocytic astrocytoma

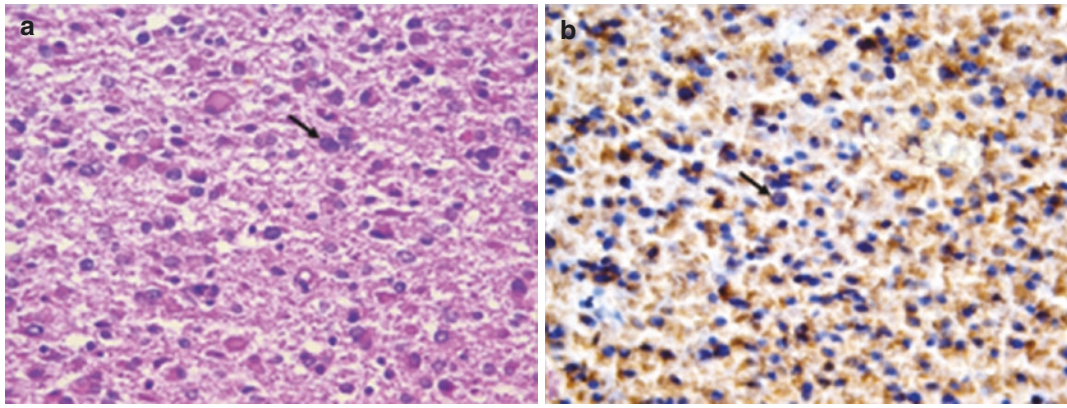

Fig. 1.1 Astrocytoma, ATRX-mutant. (**a**) H+E, ×100, tumor cells with oval nuclei (arrow) scattered in gliofibrillary matrix. (b) ATRX, ×400, loss of nuclear immunoexpression of ATRX in tumor cells (arrow)

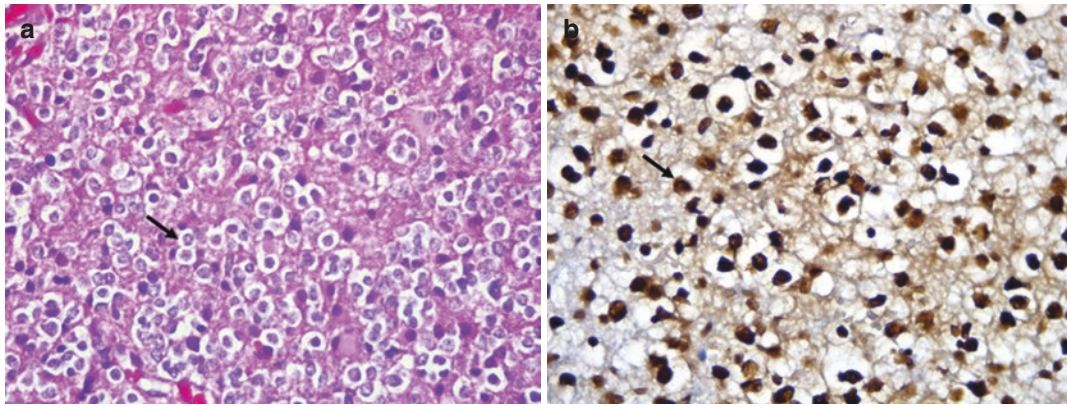

Fig. 1.2 Oligodendroglioma, ATRX-intact. (**a**) H+E, ×100, tumor cells showing typical (fried egg appearance) clear perinuclear halo of oligodendroglioma (arrow). (**b**) ATRX, ×400, immunoexpression of ATRX in tumor cells identified by nuclear brown color (arrow)

droglial gliomas, and IDH-mutant glioblastomas (secondary glioblastomas) are the R132H mutation [13]. The presence of this mutation can be detected by using an antibody for the specific gene product, immunohistochemically. The majority of diffuse astrocytomas and oligodendrogliomas demonstrate immunopositivity with the aforementioned antibody specific for R132H mutation, whereas the majority of glioblastomas (primary glioblastomas) are immunonegative [7]. Figures 1.3d and 1.4d show immunohistochemical staining with the specific R132H-mutant IDH1 antibody for an oligodendroglioma and a primary glioblastoma, respectively, along with their typical hematoxylin and eosin (H+E) stained sections and radiologic images. However, immunonegativity for R132H-mutant IDH1 antibody seen in diffuse gliomas does not rule out diffuse astrocytoma or oligodendroglioma since less common IDH1 and IDH2 mutations cannot be detected with the R132H-mutant IDH1 antibody. Assessment of IDH mutation status requires sequencing analysis for IDH1 codon 132 and IDH2 codon 172 mutations in cases that are immunohistochemically negative for the IDH1 R132H mutation. IDH-wild-type designation involves full assessment of IDH sequence analysis in addition to negative R132H-mutant IDH1 immunohistochemistry for diffuse astrocytomas and oligodendrogliomas after exclusion of other

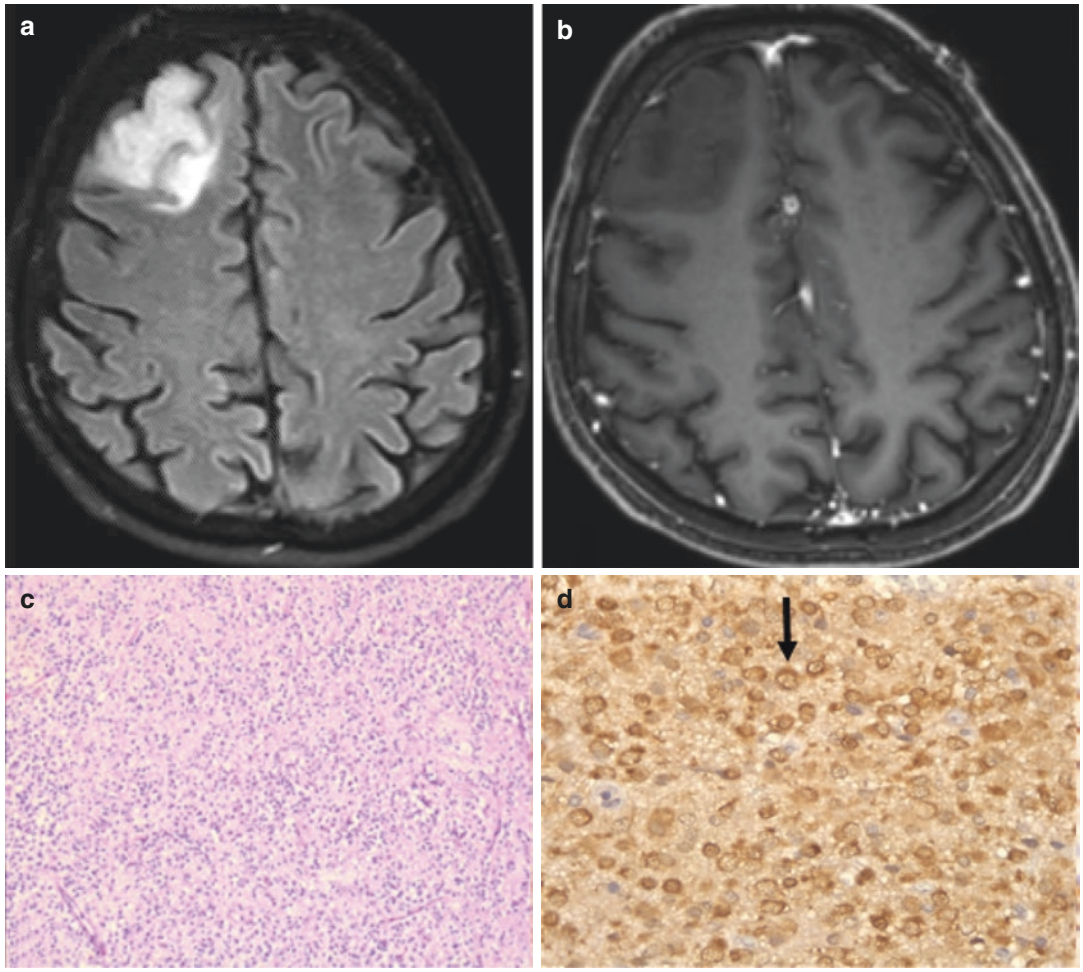

Fig. 1.3 Oligodendroglioma, IDH-mutant and 1p/19q codeleted. (**a**) Axial FLAIR MR image shows a peripherally located left temporal lobe heterogeneous hyperintense tumor with hemorrhagic signals and perifocal edema. (**b**) Axial T1-weighted contrast-enhanced MR image shows a well-defined hypointense nonenhancing mass in the right frontal lobe. (**c**) H+E, ×100, round uniform tumor cells with clear cytoplasm. (**d**) IDH1, ×400, immunoexpression of R132-mutant IDH1 protein in oligodendroglioma cells, identified by cytoplasmic brown color (arrow)

possible diagnoses. Nevertheless, IDH-wild-type designation can be applied to glioblastomas particularly in patients older than 54 years of age who do not have a lower-grade precursor lesion, without the need for IDH sequencing in the setting of negative IDH1 immunohistochemistry as proposed by Chen et al. [14].

Mutations in the IDH 1/2 genes cause overproduction of the oncometabolite 2-hydroxygluterate (2HG) within the tumor cells. 2HG can be detected by using magnetic resonance spectroscopy (MRS), albeit its routine use for this purpose is currently available only at a few institutions [15]. This modality has advantages over its alternatives in that genetic sequencing requires tissue containing at least 20% mutant alleles to be able to detect mutations on IDH1/2 [16], is time-consuming, expensive, and surrogate R132H-mutant IDH1 immunohistochemistry has false-negative results in gliomas harboring non-R132H IDH1 mutations. Besides, the availability of the information on the IDH mutation status before surgery

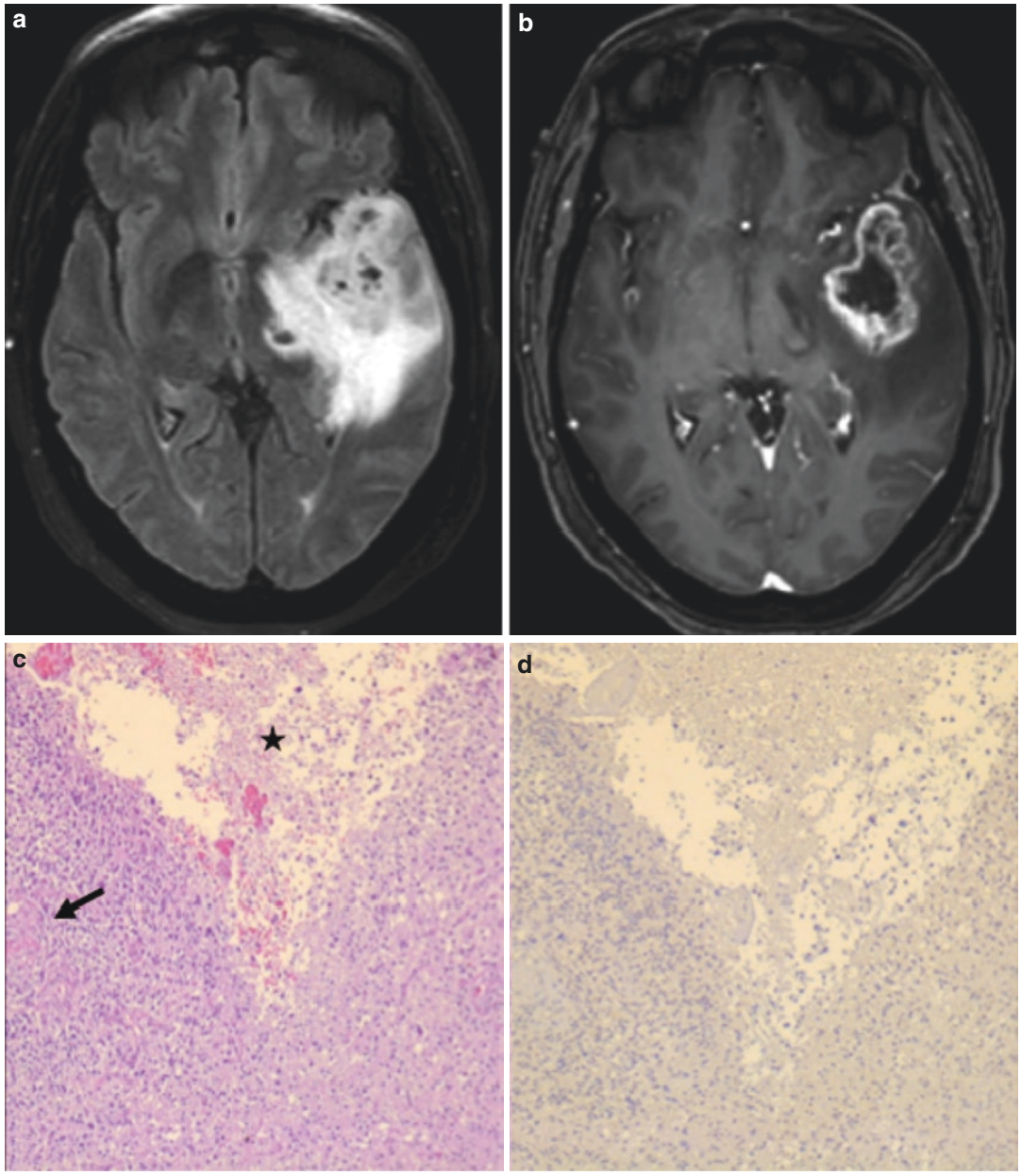

Fig. 1.4 Glioblastoma, IDH-wild type. (**a**) Axial FLAIR MR image shows a peripherally located left temporal lobe heterogeneous hyperintense tumor with hemorrhagic signals and perifocal edema. (**b**) Axial T1-weighted contrast-enhanced MR image shows irregular peripheral enhancement with central necrosis. (**c**) H+E, ×100, focus of ischemic necrosis (star) surrounded by densely accumulated tumor cells and microvascular proliferation (arrow). (**d**) IDH1, ×100, absence of R132-mutant IDH1 protein immunoexpression in tumor cell cytoplasms

is important not only for predicting prognosis but also for surgical decision-making and planning for neurosurgeons as well. In this regard, the ability to identify the IDH mutations in diffuse astrocytic and oligodendroglial tumors in the preoperative period would put the radiologists in a more critical position in the management of these patients.

1.4.2 Medulloblastomas

These tumors are classified according to their molecular characteristics based on transcriptome or methylome profiling as well as histological features. Histologically defined medullobastoma types including classic, desmoplastic/nodular, extensive nodular, and large cell/anaplastic (LCA) variants are maintained in the classification owing to its clinical usefulness when molecular tests are not available. Besides, these morphological variants have significant clinical associations. Genetically, medulloblastomas are divided into four principal subtypes: WNT (wingless)-activated, SHH (sonic hedgehog)-activated, group 3, and group 4. Histologically and genetically defined medulloblastomas show particular relationships. As a result, by combining their histological and molecular features through an integrative approach, the predictive and prognostic value of the pathological assessment increases. For instance, WNT-activated medulloblastomas with classic histological morphology have an excellent prognosis.

Although specific data is not available for each group of genetically defined medulloblastomas, some reports indicate that they have a tendency to arise in certain localizations [17, 18]. WNT-activated tumors tend to arise in the cerebellar midline/cerebellopontine angle, whereas SHH-activated tumors predominantly occur in the lateral cerebellar hemisphere and may involve the vermis. On the other hand, non-WNT/non-SHH medulloblastomas tend to present as midline tumors. By taking these into account, radiologists may predict the subtype of genetically defined medulloblastomas preoperatively.

Molecular analysis is still the gold standard in defining the genetic subgroups; however, several immunohistochemical antibodies have been found to be beneficial as surrogate markers in distinguishing WNT, SHH, and non-WNT/non-SHH medulloblastomas [19]. Nuclear β-catenin immunoreactivity is seen only in WNT-activated medulloblastomas while cytoplasmic GAB1 immunoreactivity is detected only in SHH-activated tumors. Non-WNT/non-SHH medulloblastomas can be distinguished from the other two groups by the presence of cytoplasmic β-catenin immunopositivity and GAB1 immunonegativity.

Likewise, given that immunohistochemistry is a reliable and widely available technology, certain immunohistochemical antibodies can be used instead of genetic tests also for the newly included entities and variants which have specific molecular alterations. The aforementioned antibodies are H3K27M, L1CAM, LIN28A, and VE1 and they are used as substitutes for genetic tests for diffuse midline glioma, RELA fusion-positive ependymoma, C19MC-altered ETMR, and epithelioid glioblastoma, respectively [6].

1.5 Advantages and Challenges of the 2016 CNS Tumor Classification

The new classification has several advantages and challenges. Assessment of genetic alterations with histological findings leads to the formation of more homogeneous and specific entities, thereby increasing diagnostic objectivity. This contributes to more accurate prediction of prognosis, improving patient management and response to targeted therapies. When taken into consideration that genetic tests are not available in many institutions, this classification is also useful in that it enables for the diagnosis to be made in the absence of molecular data. Classifying pediatric diffuse glial tumors that have similar morphology but different genetic features from their adult counterparts separately is a novel approach of this classification, which is likely to bring convenience for diagnosis and treatment.

Although a number of immunohistochemical surrogates are proposed by this new classification, specific assignment of certain assays as alternatives for the emphasized genetic tests is lacking in the classification. Therefore, higher interobserver variability in testing and reporting arises as a challenge of this classification. Nevertheless, with the increasing availability, reproducibility, and reliability of surrogate immunohistochemical antibodies, this challenge

is likely to be overcome in the near future. Since the integrative approach combining genotype and phenotype allows high diagnostic precision by forming more homogenous and narrower diagnostic groups, the tumors that do not fit into these categories are placed in "NOS" groups, which are essentially heterogenous "wastebasket" groups. On the other hand, these heterogeneous groups would likely serve as a source of future genetic studies aiming to improve the accuracy of the classification systems.

References

1. de Robles P, Fiest KM, Frolkis AD, Pringsheim T, Atta C, St Germaine-Smith C, et al. The worldwide incidence and prevalence of primary brain tumors: a systematic review and meta-analysis. Neuro-Oncology. 2015;17(6):776–83. https://doi.org/10.1093/neuonc/nou283.
2. Zülch KJ. Histological typing of tumours of the central nervous system. Geneva: World Health Organization; 1979.
3. Kleihues P, Burger PC, Scheithauer BW. Histological typing of tumours of the central nervous system. 2nd ed. Berlin: Springer; 1993.
4. Kleihues P, Cavenee WK. World Health Organization classification of tumours-pathology and genetics. Tumours of the nervous system. Lyon: IARC; 2000.
5. Louis DN, Ohgaki H, Wiestler OD, Cavenee WK, editors. WHO classification of tumours of the central nervous system. 4th ed. IARC: Lyon; 2007.
6. Louis DN, Ohgaki H, Wiestler OD, Cavenee WK, editors. WHO classification of tumours of the central nervous system. Revised 4th ed. Lyon: IARC; 2016.
7. Sanson M, Marie Y, Paris S, Idbaih A, Laffaire J, Ducray F, et al. Isocitrate dehydrogenase 1 codon 132 mutation is an important prognostic biomarker in gliomas. J Clin Oncol. 2009;27(25):4150–4. https://doi.org/10.1200/JCO.2009.21.9832.
8. Louis DN, Perry A, Burger P, Ellison DW, Reifenberger G, von Deimling A, et al. International Society of Neuropathology: Haarlem consensus guidelines for nervous system tumor classification and grading. Brain Pathol. 2014;24(5):429–35. https://doi.org/10.1111/bpa.12171.
9. Ellison DW, Kocak M, Figarella-Branger D, Felice G, Catherine G, Pietsch T, et al. Histopathological grading of pediatric ependymoma: reproducibility and clinical relevance in European trial cohorts. J Negat Results Biomed. 2011;10:7. https://doi.org/10.1186/1477-5751-10-7.
10. Figarella-Branger D, Civatte M, Bouvier-Labit C, Gouvernet J, Gamberelli D, Gentet JC, et al. Prognostic factors in intracranial ependymomas in children. J Neurosurg. 2000;93(4):605–13. https://doi.org/10.3171/jns.2000.93.4.0605.
11. Pajtler KW, Witt H, Sill M, Jones DT, Hovestadt W, Kratochwil F, et al. Molecular classification of ependymal tumors across all CNS compartments, histopathological grades, and age groups. Cancer Cell. 2015;27(5):728–43. https://doi.org/10.1016/j.ccell.2015.04.002.
12. Ohgaki H, Kleihues P. The definition of primary and secondary glioblastoma. Clin Cancer Res. 2013;19:764–72. https://doi.org/10.1158/1078-0432.CCR-12-3002.
13. Yan H, Parsons DW, Jin G, McLendon R, Rasheed BA, Yuan W, et al. IDH1 and IDH2 mutations in gliomas. N Engl J Med. 2009;360(8):765–73. https://doi.org/10.1056/NEJMoa0808710.
14. Chen L, Voronovich Z, Clark K, Hands I, Mannas J, Walsh M, et al. Predicting the likelihood of an isocitrate dehydrogenase 1 or 2 mutation in diagnosis of infiltrative glioma. Neuro-Oncology. 2014;16(11):1478–83. https://doi.org/10.1093/neuonc/nou097.
15. Pope WB, Prins RM, Albert Thomas M, et al. Non-invasive detection of 2-hydroxyglutarate and other metabolites in IDH1 mutant glioma patients using magnetic resonance spectroscopy. J Neurooncol. 2012;107(1):197–205. https://doi.org/10.1007/s11060-011-0737-8.
16. Arita H, Narita Y, Matsushita Y, Fukushima S, Yoshida A, Takami H, et al. Development of a robust and sensitive pyrosequencing assay for the detection of IDH1/2 mutations in gliomas. Brain Tumor Pathol. 2015;32:22–30. https://doi.org/10.1007/s10014-014-0186-0.
17. Gibson P, Tong Y, Robinson G, Thompson MC, Currle DS, Eden C, et al. Subtypes of medulloblastoma have distinct developmental origins. Nature. 2010;468(7327):1095–9. https://doi.org/10.1038/nature09587.
18. Teo WY, Shen J, Su JM, Yu A, Wang J, Chow WY, et al. Implications of tumor location on subtypes of medulloblastoma. Pediatr Blood Cancer. 2013;60(9):1408–10. https://doi.org/10.1002/pbc.24511.
19. Ellison DW, Dalton J, Kocak M, Nicholson SL, Fraga C, Neale G, et al. Medulloblastoma: clinicopathological correlates of SHH, WNT, and non-SHH/WNT molecular subgroups. Acta Neuropathol. 2011;121(3):381–96. https://doi.org/10.1007/s00401-011-0800-8.

2 When and How to Use Imaging in Brain Tumors, Protocols

Murat Alp Öztek

2.1 Introduction

Modern imaging techniques are the primary means of diagnosis of brain tumors [1]. They are also used to decide on best treatment options based on possible tumor grade, plan biopsy and surgery, evaluate extent of tumor resection, assess response to treatment, and detect recurrence.

This chapter will provide an overview of when to use imaging for brain tumors, a general overview of follow-up imaging, criteria used to assess treatment response, and recommended protocols. While the use of advanced imaging methods will be mentioned and some aspects of conventional MRI sequences will be discussed, these will be in the context of their utility in general terms. Details regarding specific uses, pearls and pitfalls of conventional sequences, and advanced imaging techniques will be discussed in other chapters of the book.

2.2 When to Use Imaging

2.2.1 Diagnosis

MRI remains the cornerstone of brain tumor imaging, and is considered the standard imaging method for diagnosis [2]. In cases where a brain tumor might be suspected, such as those with chronic headache with new features or increasing frequency, new onset headache with optic disc edema, nontraumatic seizure in patients older than 40 or with focal neurologic deficit, the most appropriate imaging is MRI with and without contrast [3, 4]. CT can be used in the emergency setting, or to look for calcification in selected patients.

While a specific histopathological diagnosis may not be possible based on the images, it is usually not needed. In many cases the distinction of low- and high-grade lesions is more important, and many patients will have biopsies or surgery for histopathologic diagnosis and molecular studies (and in case of surgery, for treatment) in any case.

2.2.2 Preoperative Planning

Surgery remains the cornerstone of treatment of brain tumors and maximum safe resection is recommended in all patients with newly diagnosed gliomas whenever feasible [2]. While some tumors in eloquent cortex or brainstem have been traditionally considered inoperable, recent advances in neurosurgery and mapping techniques make it possible to operate on at least some of those lesions [5].

In certain cases, biopsy may be preferred before (or instead of) surgery. It is well known

M. A. Öztek (✉)
Department of Radiology, University of Washington Medical Center, Seattle, WA, USA

Y. Özsunar, U. Şenol (eds.), *Atlas of Clinical Cases on Brain Tumor Imaging*,
https://doi.org/10.1007/978-3-030-23273-3_2

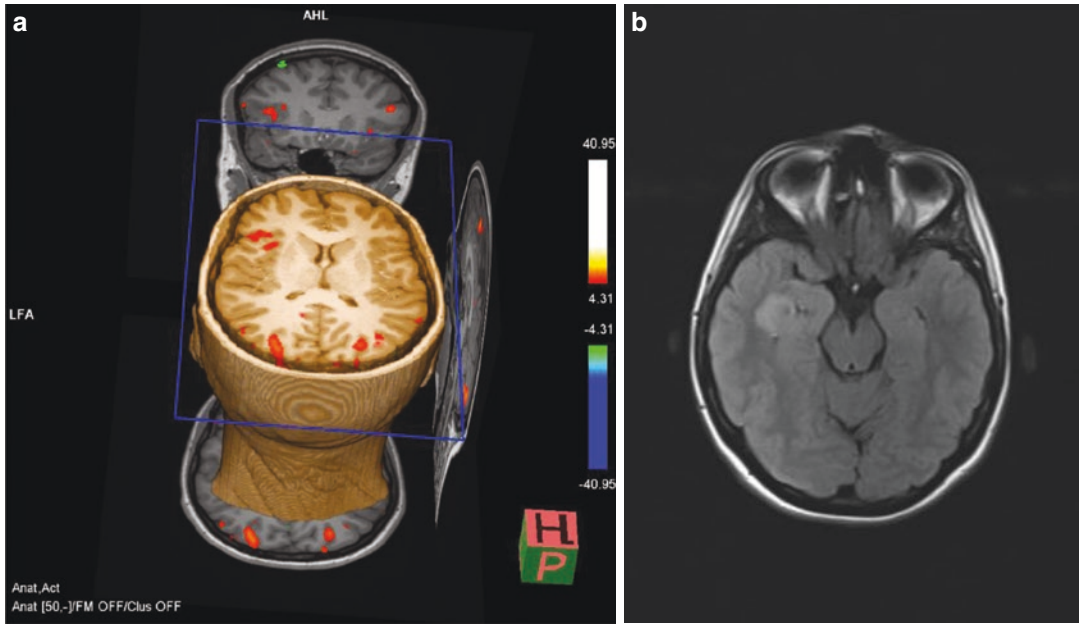

Fig. 2.1 fMRI study (**a**) to determine the location of the Broca area and plan surgery accordingly in a patient with a right temporal mass (**b**). The Broca region is demonstrated to be on the left side, which would have been impossible to determine with conventional MRI

that the heterogeneity of gliomas can cause undergrading and misdiagnosis due to sampling errors in biopsy [6]. In such patients, advanced imaging techniques can be used to target specific regions of interest to potentially improve diagnostic accuracy [6, 7].

MRI is also used in preoperative planning for navigational purposes. This is usually done with contrast-enhanced 3D-SPGR sequences that allow for high resolution and easy distinction of the tumor due to contrast enhancement. Coupled with some fiducials placed on the patient's head before the imaging study, these images can be used for intraoperative navigation. Imaging with head frames can also be performed for the same purpose in stereotactic radiosurgery or frame-based stereotactic biopsy.

Another factor with potential impact on surgery is the relation of the lesion to eloquent brain and critical white matter tracts [8]. Conventional anatomic MR imaging is insufficient to provide this information; for instance, while one can easily tell if a lesion is in the motor cortex provided one knows where the motor cortex is in that patient; brain mapping is not generalizable and must be done in a patient specific manner [9]. Functional MRI can be used to evaluate the location of the lesion with respect to eloquent brain (Fig. 2.1). The relationship of white matter tracts with the tumor can be delineated using diffusion tensor imaging (DTI) [8, 10]; thus DTI can also help improve tumor resection [11] and reduce the risk of new postoperative neurological deficits [12].

2.2.3 Intraoperative Imaging

Intraoperative MRI (iMRI) scans are beginning to get more widespread. The extent of resection is one of the factors improving overall survival in patients with gliomas [13] and use of intraoperative imaging makes it easier to ensure that as much of the lesion as is surgically feasible has been taken out [2]. This allows immediate further resection in the same session [14] and improved overall survival and progression-free survival have been reported by some groups [15, 16]. Despite these apparent benefits, there is a high cost of installation and an increase in the

healthcare cost and length of surgery [13]. There are also few studies providing high-quality evidence and evaluating whether the use of iMRI translates to improved progression-free survival or overall survival [14].

2.2.4 Postoperative Imaging

In the immediate postoperative period, unless there are operative complications or clinical concern, imaging is usually performed to determine the extent of tumor resection. In this situation, MRI is the modality of choice, provided the patient is clinically stable and there are no contraindications to an MRI scan.

Post-op imaging is also required to act as a baseline for further follow-up. The most appropriate time for baseline imaging to evaluate residual tumor is considered to be within 24–48 h of surgery and no later than 72 h [2, 17, 18]. Diffusion-weighted imaging (DWI) can also be included in the baseline imaging to determine if any future enhancement would be due to recurrence or ischemia related to surgery [18]. However, it should be noted that RANO criteria for diffuse low-grade gliomas recommend the baseline postoperative images to be preferably acquired 2–3 months after the surgery to minimize the effects of postsurgical changes such as edema, ischemia and enhancement and to better evaluate the extent of resection of non-enhancing tumors [19].

2.2.5 Follow-Up Imaging

There are two different scenarios where follow-up imaging is performed: To follow up the lesion after treatment for recurrence or progression of any non-resected parts of the mass; and to follow up lesions that did not receive any treatment. While the imaging protocol is similar in both cases, the distinction is important since it changes the differential diagnosis: new enhancement in a lesion that has been treated with chemoradiotherapy might be due to tumor progression as well as pseudoprogression or radiation necrosis in the appropriate timeframe, whereas the same change in a tumor that has not been treated would be very alarming for tumor progression.

Follow-up imaging should be performed using the same imaging modality as the baseline, which would be MRI in almost all cases [20]. Ideally, the same MRI scanner should be used, but if that is not possible or feasible, at least scanners with same magnet strength should be used (Fig. 2.2) [20].

Some clinical data can help with the interpretation of follow-up images: Type of treatment the patient received and when the treatment was completed would help determine if increasing or new enhancement could be due to pseudoprogression, radiation necrosis, or tumor progression; antiangiogenic therapy might cause decreased enhancement without true regression; changes in steroid dose can affect the size of T2/FLAIR hyperintense component and enhancement; knowledge of the radiation field could help differentiate progression or new disease outside the field from radiation-induced changes [17].

Edema, treatment-related changes, and postoperative gliosis surrounding the surgical cavity might make it difficult to determine the recurrence of the lesion using T2W or FLAIR images. Outside of the timeframe for treatment-related changes, increases in T2/FLAIR hyperintensity should be suspicious for progression of non-enhancing tumor or increasing edema. Similarly new or increasing contrast enhancement, especially outside the high-dose radiation zone, is also a red flag [17].

2.2.5.1 Pseudoprogression

Pseudoprogression is a temporary, new, or increased area of contrast enhancement without true tumor progression, caused by treatment-induced changes [21–23]. It has been described in 10–30% of GBM patients who receive radiotherapy and temozolomide, in GBM patients receiving immunotherapy, and in LGG patients receiving radiotherapy [21, 22, 24]. It occurs most commonly within 3–6 months following therapy [17, 25]. Pseudoprogression may be more frequent in patients with MGMT promoter

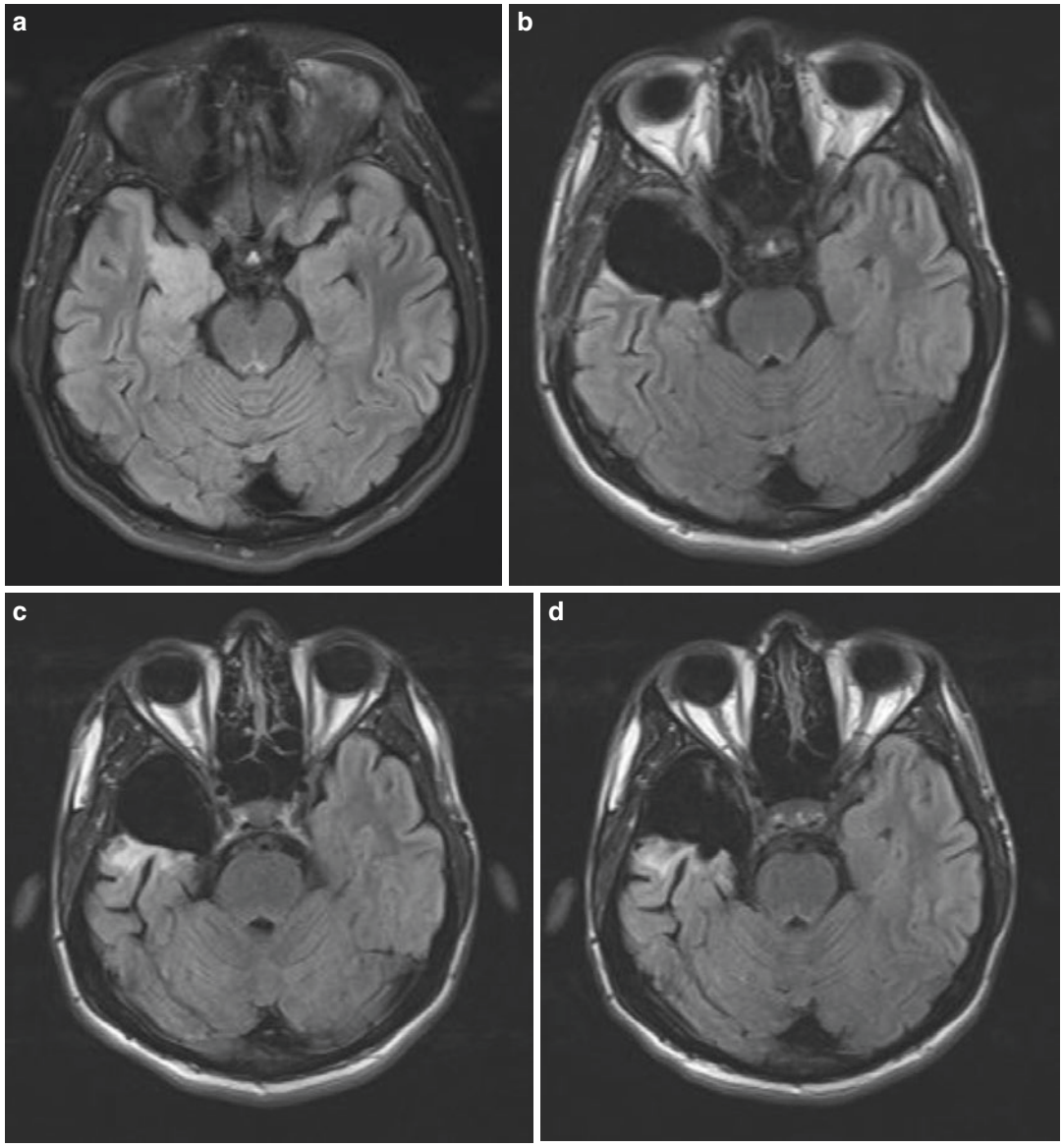

Fig. 2.2 Preoperative and follow-up FLAIR images of a 21-year-old (at time of four year follow-up) male patient with grade II glioma. (**a**) Preoperative, (**b**) 3 months post-op, (**c**) one year post-op, (**d**) four years post-op. Note the changes in FLAIR intensities surrounding the operation cavity, corresponding to gliosis

hypermethylation [17, 22]. Although most patients are asymptomatic, there may be deterioration in neurologic status or an increased need for steroids [22]. It typically resolves spontaneously [21].

Differentiating pseudoprogression from true tumor progression is challenging [24, 26]. Multifocality, the signal abnormality extending across the corpus callosum and subependymal involvement are suggestive of true progression, but there are no definitive conventional MRI findings to rule out true progression reliably [24]. Higher ADC values and lower perfusion parameters have been observed in pseudoprogression compared to true tumor progression [23, 24]; however, the thresholds reported in the literature

should be applied with care [23]. Clinical data can also help with the differential diagnosis: pseudoprogression occurs up to 6 months after treatment, and changes are expected to stabilize or improve in follow-up without any treatment [17, 24].

2.2.5.2 Radiation Necrosis

Another difficulty is radiation necrosis in patients who underwent radiotherapy. Radiation necrosis most commonly occurs 9–12 months after treatment but can be seen years after radiotherapy [17, 22]. Differentiating radiation necrosis from tumor progression is difficult using conventional MRI [17, 27]. Perfusion MRI might be helpful, but there is significant disparity in published results [17].

2.2.5.3 Pseudoresponse

Pseudoresponse or pseudoregression is a decrease in enhancement without a true antitumor effect [17, 22]. It is seen in 20–60% of patients receiving antiangiogenic therapy such as bevacizumab or cediranib and thought to be due to a normalization of abnormally permeable blood vessels which can cause marked decrease in contrast enhancement and peritumoral edema as early as day 1 after treatment [21, 24]. To distinguish this from true antitumor effect, patients under antiangiogenic therapy who demonstrate marked reduction in enhancement need to have another scan at least 4 weeks later to confirm the persistence of changes [18, 28]. Antiangiogenic therapies may select for hypoxic and invasive tumor that first grows as a non-enhancing mass before progressing to enhancing disease [24]. Therefore, careful consideration of T2/FLAIR intense non-enhancing parts of the mass is essential in this subset of patients.

2.3 Evaluating Treatment Response

In patients who underwent treatment, there is an obvious need to report whether the disease is stable, progressing, or regressing in follow-up studies. One way of doing this is simply reporting measurements and/or a subjective assessment by the radiologist. An alternative is creating an objective set of criteria to determine the response to treatment as well as provide a common terminology to be used in radiology reports. This would be beneficial especially for research purposes; however, easy-to-use, consistent, and objective terminology would certainly be useful in daily clinical practice as well. While RECIST criteria are widely used to this end for solid tumors in the body, different sets of rules are used for brain tumors [29].

The first set of such criteria was published by Levin et al. in 1977, followed by WHO oncology response criteria published in 1981 [30, 31]. The more widely used and well-known criteria (commonly referred to as Macdonald criteria) based on CT images, but later extrapolated to MRI, was proposed by Macdonald et al. in 1990. In the paper, the state of the tumor was described as complete response (CR), partial response (PR), stable disease (SD), or progression (progressive disease, PD) (Table 2.1) [32].

However, some limitations of the Macdonald criteria became apparent over time, such as not accounting for pseudoprogression, not evaluating non-enhancing component of the tumor, failing to address pseudoresponse in patients using antiangiogenic treatment, difficulty of measuring irregularly shaped tumors as well as in measuring enhancing lesions located on the walls of cysts or surgical cavities [18, 33]. To address these issues, Response Assessment in Neuro-Oncology (RANO) criteria for high-grade gliomas (RANO-HGG) was proposed in 2010 [18]. These criteria, commonly referred to as the RANO criteria, consider radiologic appearance, corticosteroid use and dose, and clinical status to define CR, PR, SD, or PD (Table 2.1). However, in the following section, only the radiographic criteria will be discussed. Interested readers are referred to the original paper for more information regarding clinical details [18].

Table 2.1 Comparison of various response assessment criteria

	RANO-HGG	RANO-LGG	RANO-BM	iRANO[g]	Macdonald
CR[a,b,d]	– No enhancement[g] – T2/FLAIR Stable to decreased[h] – No new lesions	– No lesion on T2/FLAIR, with complete resolution of enhancement if present before – No new T2/FLAIR abnormalities besides radiation effect – No new/increased enhancement – No new lesion	– No target lesions[j] – No non-target lesions[k] – No new lesions	Same as RANO-HGG, RANO-LGG or RANO-BM based on the type of tumor except for early progression[m]	– No enhancing disease – No new lesion
PR[a,c,d]	– ≥50% decrease in enhancing lesion[g,i] T2/FLAIR Stable to decreased[h] – No new lesions	– ≥50% decrease on T2/FLAIR[i] – No new T2/FLAIR abnormalities besides radiation effect – No new/increased enhancement – No new lesion	– ≥30% decrease in target lesions[j,l] – Stable or improved non-target lesions[k] – No new lesions	Same as RANO-HGG, RANO-LGG or RANO-BM based on the type of tumor except for early progression[m]	– ≥50% decrease in enhancing lesion[i] – No new lesions
SD[a,c,d]	– Enhancing lesion <50% decrease or <25% increase[i] – T2/FLAIR Stable to decreased[h] – No new lesions	– Stable on T2/FLAIR (not qualifying for other categories)[i] – No new T2/FLAIR abnormalities besides radiation effect – No new/increased enhancement – No new lesion	– Between <30% decrease and <20% increase in target lesions[j,l] – Stable or improved non-target lesions[k] – No new lesions	Same as RANO-HGG, RANO-LGG or RANO-BM based on the type of tumor except for early progression[m]	– Enhancing lesion <50% decrease or <25% increase[i] – No new lesions
PD[e,f]	– Enhancing lesion ≥25% increase[i] – Increased T2/FLAIR[h] – New lesion	– ≥25% increase on T2/FLAIR[i] – Increase in enhancement – New lesion	– ≥20% increase in target lesions[j,l] – Unequivocal progression of non-target lesions[k] – New lesion	Same as RANO-HGG, RANO-LGG or RANO-BM based on the type of tumor except for early progression[m]	– Enhancing lesion ≥25% increase[i] – New lesion
Minor Response	N/A	– 25–50% decrease on T2/FLAIR[i] – No new T2/FLAIR abnormalities besides radiation effect – No new/increased enhancement – No new lesion	N/A	If the tumor is LGG, same as RANO-LGG except for early progression[m]	N/A

BM brain metastases, *CR* complete response, *HGG* high-grade glioma, *iRANO* immunotherapy response assessment in neuro-oncology, *LGG* low-grade glioma, *PD* progressive disease, *PR* partial response, *RANO* response assessment in neuro-oncology, *SD* stable disease. Adapted from the relevant references for RANO-HGG, RANO-LGG, iRANO, RANO-BM, and Macdonald criteria [18, 19, 32, 34, 35]

[a]Patient should have all findings to qualify for the category

[b]CR requires the patient to be off corticosteroids or on physiologic replacement dose only

[c]PR and SD require the patient to be at the same or decreased corticosteroid dose compared to baseline scan

[d]CR, PR, and SD require the patient to be stable or improved clinically

Table 2.1 (continued)

[e]Any one of the findings is sufficient to qualify for progression. Neurologic deterioration not attributable to another cause also qualifies for PD by itself. Increase in corticosteroid dose by itself does not constitute PD

[f]To differentiate pseudoprogression from true tumor progression, unless progression is clearly outside the radiation field or there is pathologic confirmation, patients cannot be categorized as having PD within the first 12 weeks after chemoradiotherapy

[g]Findings should persist on a follow-up scan at least 4 weeks later

[h]Significant increase as determined qualitatively

[i]Lesion size measured as longest perpendicular two dimensions on an axial slice and multiplied. If there is more than one lesion, up to five lesions are chosen as described in the RANO-HGG section of the text and products of all lesions are summed to get a single value for comparison

[j]A measurable lesion is a contrast-enhancing lesion that can be accurately measured in at least one dimension, with a minimum size of 10 mm (or twice the slice thickness). The diameter perpendicular to the longest dimension should at least be 5 mm. Up to five largest measurable lesions that can be measured reproducibly can be picked as target lesions. Lesions not treated with local therapies are preferred if present

[k]All measurable lesions besides target lesions and all non-measurable lesions are non-target lesions. They should be recorded at baseline and classified as present, absent or unequivocal progression in follow-up

[l]Only the largest diameter in an axial slice is measured. In cases of multiple target lesions, the diameters are summed to get a single value for comparison in follow-up

[m]If there is radiological progression of lesions within 6 months of starting immunotherapy (including presence of new lesions), follow-up imaging is required 3 months later. If 3-month follow-up scan meet the criteria for CR, PR, or SD then the patient is categorized thus. If the 3-month follow-up scan demonstrates PD, the patient is considered to have PD. If there are new or increasing neurological symptoms not attributable to comorbid events in this time period, the patient is deemed to have PD. If radiological progression occurs more than 6 months after starting immunotherapy, the patient is considered to have PD and 3-month follow-up scan is not required for categorization

2.3.1 Response Assessment in Neuro-Oncology: High-Grade Glioma (RANO-HGG)[1]

RANO-HGG criteria (commonly referred to as only the "RANO criteria") define measurable disease as bidimensionally contrast-enhancing lesion(s) with clearly defined margins on CT or MRI, with two largest perpendicular diameters on an axial slice being at least 10 mm (Fig. 2.3). The lesion should be visible on at least two consecutive axial slices, and the slice thickness must preferably be at most 5 mm with 0 mm gap. If the slice thickness is greater than 5 mm, the size of the lesion should be at least two times the slice thickness to be considered measurable. If the lesion is unidimensionally measurable, lacks clearly defined margins, or smaller than 10 mm (or twice the slice thickness) in at least one dimension, it should be considered nonmeasurable. Special note is made of tumors around a cyst or surgical cavity: such lesions are to be considered nonmeasurable unless they have a clear nodular component that satisfies criteria for being measurable (i.e., at least 10 mm in two perpendicular dimensions).

If there is more than one lesion, two to five of the largest lesions should be measured in two dimensions, the area should be calculated as the product of the two diameters and then the areas of the measured lesions should be added to get a single final value. Comparisons in follow-up should be made using this single value. While typically the largest lesions are selected for measurement, care should be taken to ensure that these lesions allow reproducible measurements. In cases where the largest lesions do not lend themselves to reproducible measurements, the next largest lesion that can be measured reproducibly can be selected instead. The lesions picked for measurement and calculation of the final value for comparison are defined to be the "target lesions."

Non-enhancing components of the tumor are evaluated using T2W or FLAIR images, where they have similar appearance to peritumoral edema and radiation-related changes, making exact delineation of its margins quite difficult.

[1]Adapted from [18].

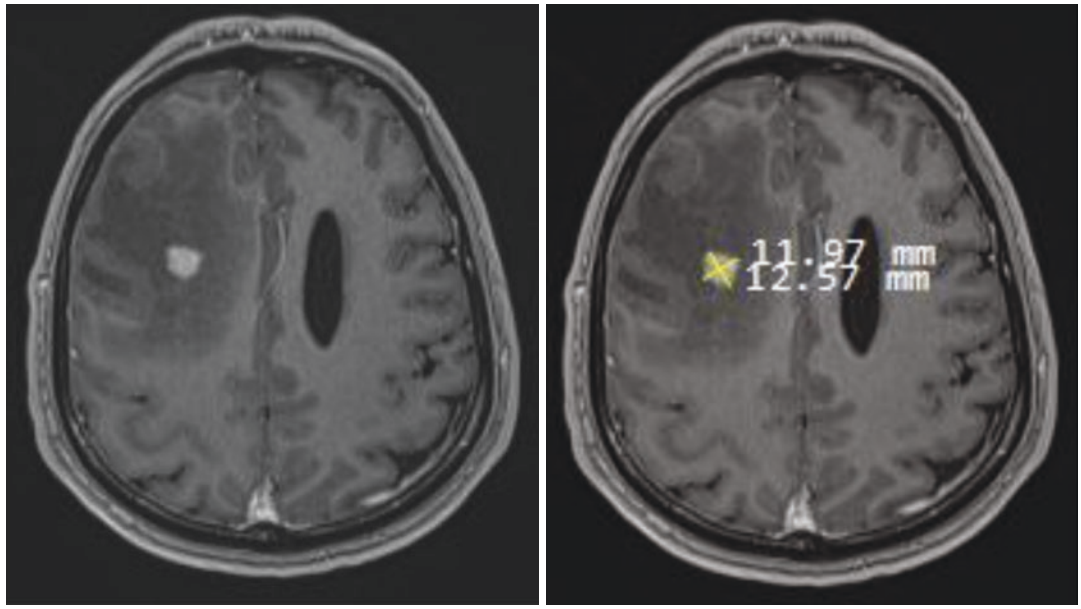

Fig. 2.3 Sample measurement of a high-grade glioma according to RANO criteria. With both dimensions of the enhancing part greater than 10 mm, this constitutes measureable disease

Signs of mass effect such as sulcal effacement or compression of the ventricles; infiltration of the cortical ribbon or simply the location being outside of the radiation field suggest infiltrating tumor. Sometimes, there might still be doubt as to whether the changes represent an increase in non-enhancing tumor. In such cases further follow-up usually confirms or refutes the idea. While objective measures of non-enhancing tumor would obviously be helpful, there are no widely accepted methods for this purpose and RANO criteria do not incorporate any such methods yet.

Response is determined in comparison to the baseline imaging to determine CR or PR, and the smallest tumor measurement (in pre-treatment baseline images or in follow-up images after the initiation of treatment) to determine PD. In cases where the changes are equivocal, close follow-up is indicated. Rules to classify response are provided in Table 2.1.

2.3.2 Other RANO Criteria

Patients receiving immunotherapy and patients with other types of brain tumors should not be evaluated using RANO-HGG criteria. There are different criteria described for brain metastases (RANO-BM), low-grade gliomas (RANO-LGG), and patients undergoing immunotherapy (iRANO) [19, 34, 35]. Major differences of these criteria and how they compare to RANO-HGG are provided in Table 2.1. Response assessment for leptomeningeal metastases (RANO-LM) is handled in a totally different manner and interested readers are referred to the original paper for details on how to score imaging data [36]. Criteria for spine tumors (SPINO), pediatric brain tumors (RAPNO), and meningiomas (RANO-meningioma) are also under development [37–39].

2.4 Imaging Protocol

To standardize neuro-oncologic imaging in clinical trials, Consensus Recommendations for a Standardized Brain Tumor Imaging Protocol (BTIP) have been reported [20]. While this protocol is concerned mostly with standardizing MRI acquisition to facilitate multicenter studies and comparison of different studies, it is also recommended to be used for routine, clinical brain tumor imaging [33]. According to BTIP, MRI

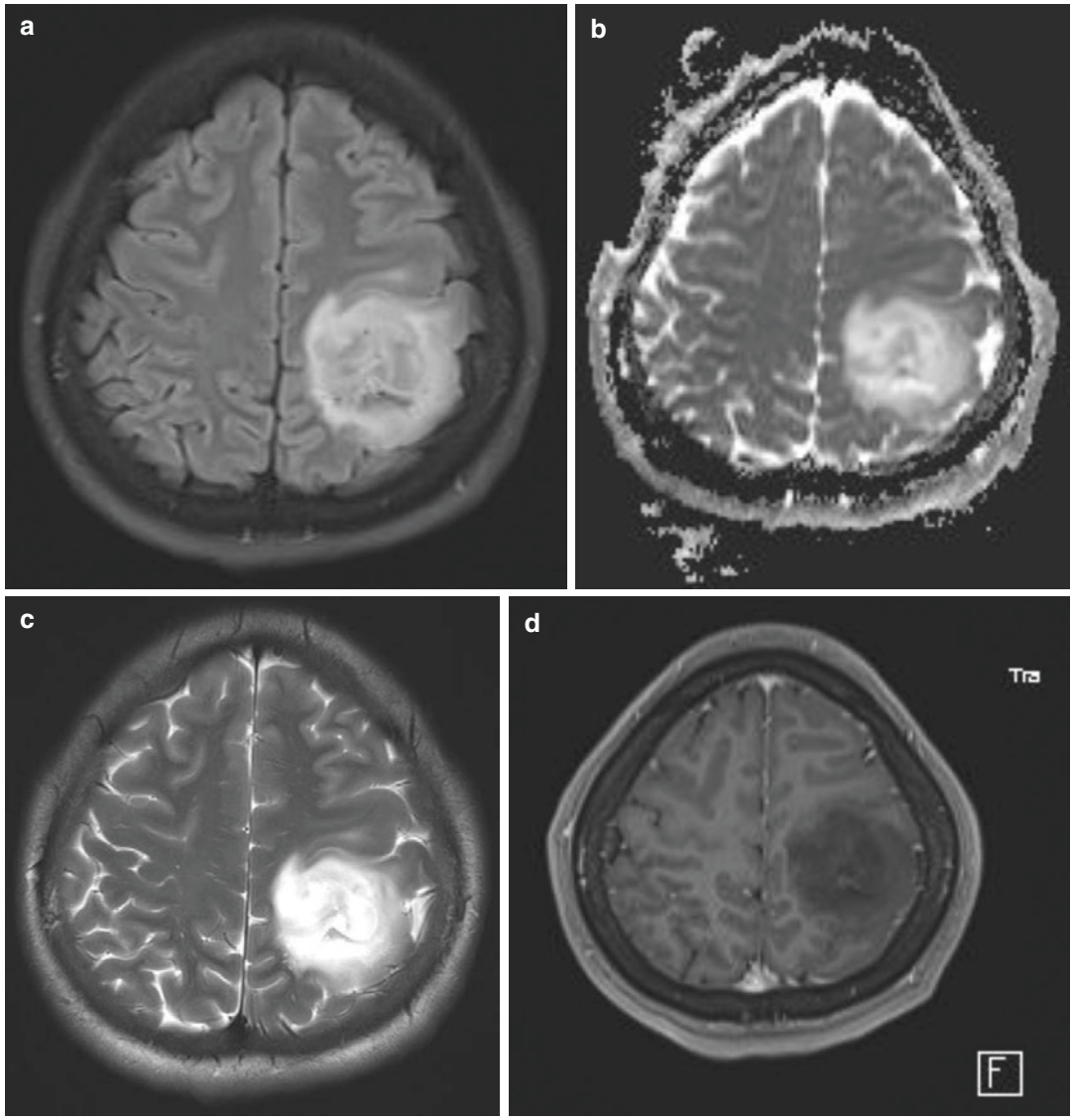

Fig. 2.4 Sample images for brain tumor imaging according to the recommended protocol: (**a**) 2D FLAIR, (**b**) ADC map acquired from DWI using 3 directions and b values 0, 500 and 1000 s/mm^2, (**c**) 2D T2W, (**d**) post-contrast 3D T1W. It should be noted that T1W images were acquired in the sagittal plane but are here demonstrated in the axial plane (using MPR) to be consistent with other images

imaging of brain tumors should include at least the following sequences (Fig. 2.4) [20]:

- Pre-contrast and post-contrast isotropic 3D inversion recovery-prepared T1W gradient-recalled echo (IR-GRE) images with matching parameters
- Axial 2D T2W TSE (dual echo preferred but not required) acquired after contrast injection but before post-contrast T1W images
- Pre-contrast axial 2D TSE T2W FLAIR
- Pre-contrast axial 2D three-directional DWI using echoplanar (EPI) or radial acquisition

The scanner used may be 1.5 T or 3 T [20]. There have been studies reported on 7 T scanners, but whether the use of 7 T scanners would translate into clinical benefit within the context of brain tumors is not clear [40]

Specific acquisition parameters as described by the consensus statements are provided in Table 2.2 [20]

Table 2.2 Consensus recommendations for a standardized brain tumor imaging protocol; recommended protocols for 3 T and 1.5 T scanners

	Pre-contrast T1W[a]		FLAIR[e]		DWI[h]		IV Contrast injection[j]	T2W[k]		Post-contrast T1W[a,l]	
Sequence	IR-GRE[b]		TSE[f]		EPI[i]			TSE[f]		IR-GRE[b]	
Plane of acquisition	Sagittal/axial[c]		Axial		Axial			Axial		Sagittal/axial[c]	
3D/2D	3D		2D		2D			2D		3D	
Field strength	3 T	1.5 T	3 T	1.5 T	3 T	1.5 T		3 T	1.5 T	3 T	1.5 T
TR (ms)	2100[d]	2100[d]	>6000	>6000	>5000	>5000		>2500	>3500	2100[d]	2100[d]
TE (ms)	Min	Min	100–140	100–140	Min	Min		80–120	100–120	Min	Min
TI (ms)	1100[d]	1100[d]	2500	2200	–	–		–	–	1100[d]	1100[d]
Flip angle	10–15°	10–15°	90°/≥160°	90°/≥160°	90°/180°	90°/180°		90°/≥160°	90° ≥ 160°	10–15°	10–15°
Frequency	256	≥172	≥256	≥256	128	128		≥256	≥256	256	≥172
Phase	256	≥172	≥256	≥256	128	128		≥256	≥256	256	≥172
NEX	≥1	≥1	≥1	≥1[g]	≥1	≥1[g]		≥1	≥1[g]	≥1	≥1
FOV (mm)	256	256	240	240	240	240		240	240	256	256
Slice thickness (mm)	1	≤1.5	3	≤4[g]	3	≤4[g]		3	≤4[g]	1	≤1.5
Gap/spacing	0	0	0	0	0	0		0	0	0	0
Parallel imaging	Up to 2×	No	Up to 2×	Up to 2×	Up to 2×	Up to 2×		Up to 2×	Up to 2×	Up to 2×	No

Adapted from [20]

DWI diffusion-weighted imaging, *EPI* echo planar imaging, *FLAIR* fluid attenuated inversion recovery, *FOV* field of view, *FSE* fast spin echo, *GRAPPA* generalized autocalibrating partial parallel acquisition, *IR-GRE* inversion recovery gradient-recalled echo, *NEX* number of excitations, *PD* proton density, *SNR* signal-to-noise ratio, *TE* echo time, *TI* inversion time, *TR* repetition time, *TSE* turbo spin echo

[a]Post-contrast T1W images should have identical parameters to pre-contrast T1W images

[b]3D acquisitions without inversion preparation should be avoided

[c]Sagittal preferred due to fewer required slices and thus shorter scan times

[d]The values provided are for Siemens and Hitachi scanners. GE, Philips and Toshiba scanners should use *TR* = 5–15 ms and *TI* = 400–450 ms

[e]3D FLAIR images are strongly endorsed, due to the possibility of multiplanar reconstruction, volumetry and less sensitivity to flow artifacts; but are considered optional due to not being universally available. The following parameters are recommended for 3D FLAIR: *TE* = 90–140 ms, *TR* = 6000–10,000 ms, *TI* = 2000–2500 ms (chosen based on vendor recommendations), GRAPPA ≤2, fat saturation, slice thickness ≤1.5 mm, FOV ≤250 mm × 250 mm, matrix ≥244 × 244, sagittal or axial acquisition

[f]TSE is equivalent to FSE in GE, Hitachi, and Toshiba scanners

[g]To get comparable SNR, older 1.5 T scanners can use images with 5 mm slice thickness with no interslice gap or increase NEX for slice thickness ≤4 mm

[h]DWI images should be acquired in at least 3 directions with $b = 0$, 500 and 1000 s/mm^2. If the scanner is an older scanner incapable of at least three b values, $b = 0$, 1000 s/mm^2 should be used

[i]If there is significant patient motion, radial acquisition schemes may be used. However, this should be a last option

[j]0.1 mmol/kg (up to 20 cc) gadolinium-chelated contrast injection at a rate of 3–5 cc/s, preferably using a power injector, as a single, full dose

[k]Dual echo PD/T2 TSE is optional. If used, the PD echo should have a TE <25 ms

[l]Advanced sequences can be substituted before the post-contrast T1W images as long as post-contrast 3D T1W sequences are acquired between 4–8 min following contrast administration